Published by Institute of Physics Publishing for SISSA/ISAS
Received: *March 21, 2002*
Revised: *April 25, 2002*
Accepted: *April 29, 2002*

Transport coefficients, spectral functions and the lattice

Gert Aarts and Jose María Martínez Resco

Department of Physics, The Ohio State University
174 West 18th Avenue, Columbus, OH 43210, USA
Email: aarts@mps.ohio-state.edu, marej@pacific.mps.ohio-state.edu

Abstract: Transport coefficients are determined by the slope of spectral functions of composite operators at zero frequency. We study the spectral function relevant for the shear viscosity for arbitrary frequencies in weakly-coupled scalar and nonabelian gauge theories at high temperature and compute the corresponding correlator in euclidean time. We discuss whether nonperturbative values of transport coefficients can be extracted from euclidean lattice simulations.

Keywords: Lattice Quantum Field Theory, Thermal Field Theory.

JHEP04(2002)053

© SISSA/ISAS 2002

Contents

JHEP04(2002)053

1. Introduction

In recent years there has been a growing interest in the calculation of transport coefficients in quantum field theories at finite temperature. With the advent of relativistic heavy-ion colliders, such as RHIC, a proper knowledge of transport coefficients has become relevant since hydrodynamical descriptions of heavy-ion collisions provide a useful tool to analyse the experimental data [1]. In practice the extension of ideal relativistic hydrodynamics to include finite transport coefficients is far from straightforward and applications to heavy-ion physics have only just begun [2].

If the temperature is sufficiently high and the theory is weakly coupled, transport coefficients can be computed in a perturbative expansion, employing either kinetic theory or field theory using Kubo formulas. It turns out that the latter approach requires the summation of an infinite series of higher-order diagrams, known as ladder diagrams, which has been a serious drawback for its use. For a scalar theory, the higher-order contributions in the loop expansion have been identified and summed in ref. [3], using an intricate diagrammatic analysis, and the leading-order results for the shear and bulk viscosities have been found. In ref. [4] the equivalence of an effective Boltzmann equation and the field-theoretical calculation is shown. Using a more transparent analysis, the diagrammatic conclusions of ref. [3] have been confirmed recently [5]. So far, the only other transport coefficient for which the ladder series has been summed explicitly is the color conductivity in QCD [6]. The viscosities in the scalar theory and color conductivity in QCD have the property that the one-loop contribution and the ladder contributions are of the same order in the coupling constant. However, for other transport coefficients in gauge theories, such as the shear viscosity or the electrical conductivity, the ladder contributions are in fact larger than the one-loop one [7]. Only recently and using kinetic theory, a complete computation of the leading logarithmic order of these transport coefficients has appeared [8]. Unfortunately, a full leading-order computation is still lacking. Ref. [8] provides a useful guide to the literature.

Euclidean lattice simulations offer in principle the possibility to compute transport coefficients completely nonperturbatively [9]. However, transport coefficients are determined by the small frequency limit of zero-momentum spectral functions of appropriate composite operators (such as components of the energy-momentum tensor) and spectral functions or other real-time correlators are not readily available on a euclidean lattice, although recent progress has been made with the Maximal Entropy Method (MEM) [10, 11].[1] For that reason it was proposed in ref. [9] to introduce instead an ansatz for the spectral function and fit the result to the numerical data for the euclidean correlator, employing a standard dispersion relation between these two. This approach was pursued more recently in refs. [13, 14].

Motivated by these studies, our goal in this paper is to compute the spectral function relevant for the shear viscosity at high temperature in weakly-coupled scalar (section 3) and nonabelian gauge theories (section 4). In the conclusions we compare our findings with the analysis carried out so far in refs. [9, 13, 14]. It is found that the ansatz used in these papers is inadequate and we suggest a better one. We also point out a potential problem in the calculation of spectral functions at very low frequencies ($\omega \to 0$) from euclidean lattice correlators using the MEM approach.

2. Correlation functions

We start with a summary of basic relations between transport coefficients, spectral functions and euclidean correlators, using the shear viscosity as an example. The relations presented in this section are quite general and valid for arbitrary transport coefficients.

The shear viscosity can be defined from a Kubo relation as

$$\eta = \frac{1}{20} \lim_{\omega\to 0} \frac{1}{w} \int d^4x\, e^{i\omega t} \left\langle [\pi_{kl}(t,\mathbf{x}), \pi_{kl}(0,\mathbf{0})] \right\rangle , \tag{2.1}$$

with π_{kl} the traceless part of the spatial energy-momentum tensor. The brackets denote the equilibrium expectation value at temperature T. We define spectral functions of hermitean (composite) operators, such as π_{kl}, as the expectation value of the commutator,

$$\rho_{\pi\pi}(x-y) = \left\langle [\pi_{kl}(x), \pi_{kl}(y)] \right\rangle , \tag{2.2}$$

and in momentum-space

$$\rho_{\pi\pi}(\omega,\mathbf{p}) = \int d^4x\, e^{i\omega t - i\mathbf{p}\cdot\mathbf{x}} \rho_{\pi\pi}(t,\mathbf{x}) . \tag{2.3}$$

Spectral functions obey basic symmetry relations[2] $\rho^*_{\pi\pi}(x) = -\rho_{\pi\pi}(x) = \rho_{\pi\pi}(-x)$ and $\rho^*_{\pi\pi}(\omega,\mathbf{p}) = \rho_{\pi\pi}(\omega,\mathbf{p}) = -\rho_{\pi\pi}(-\omega,\mathbf{p})$ as well as the positivity condition $\omega\rho_{\pi\pi}(\omega,\mathbf{p}) \geq 0$.

[1] Note that for classical field theories at finite temperature spectral functions can be computed nonperturbatively by numerical simulations directly in real time [12].

[2] When most manipulations take place in real-space, it can be convenient to define spectral functions such that they are real instead of purely imaginary in real-space. Here we stick to the usual convention and spectral functions are real in momentum-space.

JHEP04(2002)053

The shear viscosity is determined by the slope at zero frequency:

$$\eta = \frac{1}{20}\frac{d}{d\omega}\rho_{\pi\pi}(\omega)\Big|_{\omega=0}\,, \tag{2.4}$$

where $\rho_{\pi\pi}(\omega) = \rho_{\pi\pi}(\omega,\mathbf{0})$. Since the spectral function is odd, we consider from now on positive ω only.

The euclidean correlator (at zero spatial momentum) is given by

$$G^E_{\pi\pi}(\tau) = \int d^3x\,\langle\pi_{kl}(\tau,\mathbf{x})\pi_{kl}(0,\mathbf{0})\rangle_E \qquad (\tau = it)\,, \tag{2.5}$$

where the imaginary time $\tau \in [0, 1/T]$ and $G^E_{\pi\pi}(1/T-\tau) = G^E_{\pi\pi}(\tau)$. The euclidean correlator and the spectral function are related via an integral equation, originating from a dispersion relation,

$$G^E_{\pi\pi}(\tau) = \int_0^\infty \frac{d\omega}{2\pi}\,K(\tau,\omega)\rho_{\pi\pi}(\omega)\,, \tag{2.6}$$

with the kernel

$$K(\tau,\omega) = e^{\omega\tau}n(\omega) + e^{-\omega\tau}\left[1+n(\omega)\right] = e^{-\omega\tau} + 2n(\omega)\cosh\omega\tau\,, \tag{2.7}$$

obeying $K(\tau,\omega) = -K(\tau,-\omega) = K(1/T-\tau,\omega)$. The Bose distribution is

$$n(\omega) = \frac{1}{\exp(\omega/T)-1}\,. \tag{2.8}$$

The low-frequency part of the spectral function contains all information on the transport coefficient and its effect on the euclidean correlator can be estimated quite easily. When $\omega \ll T$, the kernel can be expanded as

$$K(\tau,\omega) = \frac{2T}{\omega} + \frac{\omega}{T}\left[\frac{1}{6} - \tau T(1-\tau T)\right] + \mathcal{O}\left(\frac{\omega^3}{T^3}\right), \tag{2.9}$$

and all except the first term are suppressed. As a consequence we find that the contribution to the euclidean correlator from low frequencies,

$$G^{E,\text{low}}_{\pi\pi}(\tau) = 2T\int_0^{\omega_\Lambda}\frac{d\omega}{2\pi}\,\frac{\rho_{\pi\pi}(\omega)}{\omega}\,, \tag{2.10}$$

is independent of τ. The frequency cutoff $\omega_\Lambda \ll T$ is introduced here to justify the expansion of the kernel. We conclude that the dominant effect of the low-frequency region is a constant τ-independent contribution to the euclidean correlator.

3. Scalar field

We consider a one-component massless scalar field with a quartic $\lambda\phi^4/4!$ interaction.[3] The one-particle spectral function is

$$\rho(x-y) = \langle[\phi(x),\phi(y)]\rangle = G^>(x-y) - G^<(x-y)\,. \tag{3.1}$$

[3] We assume that the temperature is sufficiently high such that a possible zero-temperature mass $m_0^2 \ll \lambda T^2$ plays no role.

JHEP04(2002)053

The one-particle Wightman functions, $G^{>}(x-y) = \langle\phi(x)\phi(y)\rangle$ and $G^{<}(x-y) = \langle\phi(y)\phi(x)\rangle$, are related to the one-particle spectral function via the KMS condition

$$G^{>}(p) = \left[n(p^0)+1\right]\rho(p)\,, \qquad G^{<}(p) = n(p^0)\rho(p)\,. \tag{3.2}$$

The traceless part of the spatial energy-momentum tensor reads

$$\pi_{kl} = \partial_k\phi\partial_l\phi - \frac{1}{3}\delta_{kl}\partial_m\phi\partial_m\phi. \tag{3.3}$$

The lowest-order skeleton diagram that contributes to the spectral function for the shear viscosity in eq. (2.2) follows from simple Wick contraction,

$$\langle[\phi^2(x),\phi^2(y)]\rangle = 2\left[G^{>2}(x-y) - G^{<2}(x-y)\right], \tag{3.4}$$

and we find

$$\rho_{\pi\pi}(\omega) = \frac{4}{3}\int\frac{d^4k}{(2\pi)^4}\,(\mathbf{k}\cdot\mathbf{k})^2 n(k^0)\rho(k^0,\mathbf{k})\left[\rho(k^0+\omega,\mathbf{k}) - \rho(k^0-\omega,\mathbf{k})\right], \tag{3.5}$$

where we used the KMS conditions (3.2) and $-n(-\omega) = n(\omega)+1$. The four $\mathbf{k}$'s in the integrand arise from the derivatives in π_{kl}. In the remainder of this section we compute the one-loop spectral function (3.5) as a function of the external frequency.

The spectral function $\rho_{\pi\pi}$ depends on the one-particle spectral functions ρ, which contain the quasiparticle structure of the theory at finite temperature. We describe this in some detail since similar, though more complicated, considerations appear in gauge theories. For hard momenta $|\mathbf{k}|\sim T$, excitations are on-shell with energy $|\mathbf{k}|$. For softer momenta screening effects become important and hard thermal loop (HTL) resummation yields a temperature-dependent plasmon mass, $m^2 = m_{\rm th}^2(1-3m_{\rm th}/\pi T+\ldots)$ with $m_{\rm th}^2 = \lambda T^2/24$ [15]. Finally, collisions in the plasma result in a finite (but narrow) momentum-dependent width $2\gamma_{\mathbf{k}} \ll m \ll T$, changing the one-particle spectral function from an on-shell delta function to a Breit-Wigner spectral function (see below) [16].

We may now discuss the one-loop expression (3.5). First we note that the integral is dominated by hard $\sim T$ momenta. Therefore, for external frequencies that are not too small a simple on-shell delta function for the one-particle spectral functions suffices to find the dominant contribution. We will refer to this region as the high-frequency region. For smaller frequencies, however, the arguments of the delta functions come close, producing a so-called pinch singularity [3]. The pinch singularity is screened by a finite external frequency or width, whichever one is the largest. For very small external frequencies, the inclusion of the width[4] is essential [3]. This situation is sketched in figure 1. The effect of these nearly pinching poles is to enhance the spectral function compared to naive estimates. We will refer to the region where pinching poles are important as the low-frequency domain.

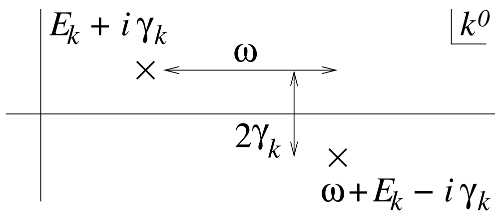

Figure 1: Typical configuration of poles in the complex k^0-plane for the evaluation of the one-loop spectral function $\rho_{\pi\pi}(\omega)$, $E_{\mathbf{k}}$ $(2\gamma_{\mathbf{k}})$ denotes the quasiparticle energy (width).

[4] And of ladder diagrams, see below.

JHEP04(2002)053

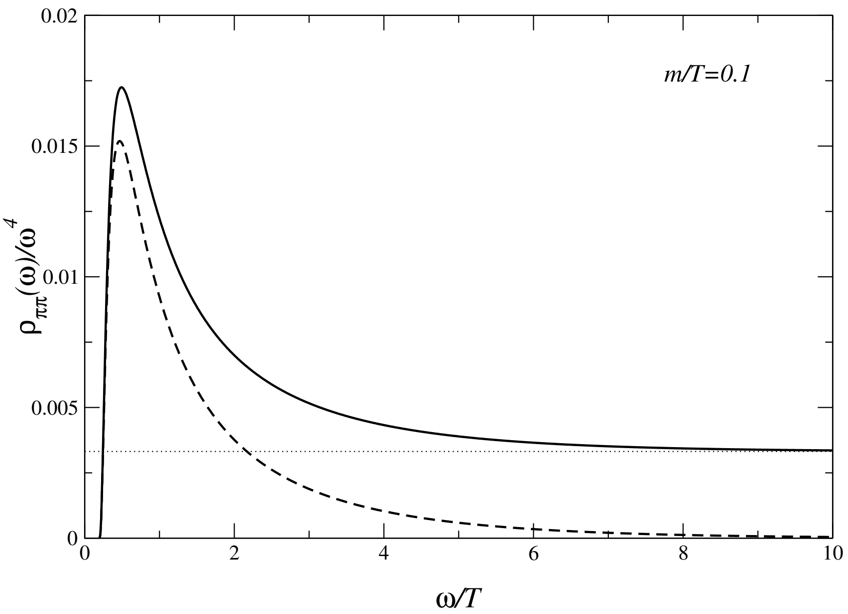

Figure 2: Contribution to the spectral function $\rho_{\pi\pi}(\omega)/\omega^4$ (full line) from decay/creation processes (see eq. (3.7)) as a function of ω/T, with $m/T = 0.1$. The contribution from the nearly pinching poles in the low-frequency region is discussed below. The dashed line shows the contribution proportional to the Bose distribution only. The dotted line indicates the asymptotic value.

We start with the region where the frequency is much larger than the thermal width and no pinch-singularity problems are encountered. The one-particle spectral function can be taken on-shell and is

$$\rho_0(k^0, \mathbf{k}) = 2\pi\epsilon(k^0)\delta(k_0^2 - \omega_{\mathbf{k}}^2)\,, \tag{3.6}$$

where $\omega_{\mathbf{k}} = \sqrt{\mathbf{k}^2 + m^2}$ and $\epsilon(x)$ the sign-function. HTL effects are included in the mass parameter. Evaluating the integrals in eq. (3.5) with the use of the delta-functions (the angular integrals are trivial) results in (recall that we take $\omega > 0$)

$$\rho_{\pi\pi}(\omega) = \theta(\omega - 2m)\frac{\left(\omega^2 - 4m^2\right)^{5/2}}{48\pi\omega}\left[n\left(\frac{\omega}{2}\right) + \frac{1}{2}\right], \tag{3.7}$$

which is shown in figure 2. The physical processes are the decay of a zero-momentum excitation with energy ω into two on-shell particles with equal and opposite momentum, and the inverse process of creation. The decay process contributes also at zero temperature and makes the spectral function increase as ω^4 at large frequencies. The threshold at $\omega = 2m$ arises from (simple) HTL resummation. This concludes the analysis of the spectral function in the high-frequency domain.

We continue with the low-frequency region where pinch singularities lead to a non-trivial enhancement of the spectral function. We replace the on-shell one-particle spectral functions with Breit-Wigner spectral functions:

$$\rho_{BW}(k^0, \mathbf{k}) = \frac{1}{2\omega_{\mathbf{k}}}\left[\frac{2\gamma_{\mathbf{k}}}{(k^0 - \omega_{\mathbf{k}})^2 + \gamma_{\mathbf{k}}^2} - \frac{2\gamma_{\mathbf{k}}}{(k^0 + \omega_{\mathbf{k}})^2 + \gamma_{\mathbf{k}}^2}\right]. \tag{3.8}$$

JHEP04(2002)053

The width $2\gamma_{\mathbf{k}}$ is determined by the imaginary part of the retarded self energy

$$\gamma_{\mathbf{k}} = -\frac{\mathrm{Im}\,\Sigma_R(\omega_{\mathbf{k}},\mathbf{k})}{2\omega_{\mathbf{k}}}\,, \tag{3.9}$$

and the dominant contribution at weak coupling arises from two-to-two scattering from the two-loop setting-sun diagram [3, 16]. A convenient way to write this damping rate is as [17]

$$\gamma_{\mathbf{k}} = \gamma\frac{T}{\omega_{\mathbf{k}}}B\left(\frac{|\mathbf{k}|}{T};\frac{m}{T}\right), \tag{3.10}$$

where

$$\gamma = \frac{\lambda^2 T}{1536\pi}\,, \tag{3.11}$$

determines the parametrical behaviour. The function B contains the nontrivial momentum dependence and is related to A defined in ref. [17] as $B(|\mathbf{k}|/T;m/T) = (6/\pi^2)\times A(|\mathbf{k}|/T;m/T)$. In the limit of hard momenta and small mass [17]

$$\lim_{m\to 0}\lim_{|\mathbf{k}|\to\infty} B\left(\frac{|\mathbf{k}|}{T};\frac{m}{T}\right) = 1\,. \tag{3.12}$$

For analytical estimates we will neglect the momentum dependence and take $B = 1$. In the results obtained by numerical integration the full momentum dependence is included.

We insert the Breit-Wigner functions into expression (3.5) for the spectral function and perform the k^0 integral by integrating around the poles in the complex plane. We preserve only the dominant contributions and discard all terms suppressed by (powers of) the coupling constant with respect to the leading order contribution. Breit-Wigner spectral functions have four poles at complex energy-arguments $k^0 = \pm(\omega_{\mathbf{k}} \pm i\gamma_{\mathbf{k}})$. From the residue of these poles we keep $n(\omega_{\mathbf{k}} \pm i\gamma_{\mathbf{k}}) \sim n(\omega_{\mathbf{k}})$. The Bose distribution $n(k^0)$ has poles along the imaginary axis at $k^0 = 2\pi i n T$, $n \in \mathbb{Z}$. However, the residues at these poles are subdominant compared to those from the poles of the Breit-Wigner functions. Hence we do not include these contributions. After performing the k^0 integral we find

$$\rho_{\pi\pi}(\omega) = -\frac{4}{3}\int_{\mathbf{k}}\frac{|\mathbf{k}|^4}{2\omega_{\mathbf{k}}}\left\{[n(\omega_{\mathbf{k}}) - n(\omega_{\mathbf{k}}-\omega)]I(\omega,\mathbf{k})\frac{\omega_{\mathbf{k}}-\omega}{\omega^2+4\gamma_{\mathbf{k}}^2} - [\omega\to-\omega]\right\}, \tag{3.13}$$

with

$$\int_{\mathbf{k}} = \int\frac{d^3k}{(2\pi)^3}\,, \tag{3.14}$$

and

$$I(\omega,\mathbf{k}) = \frac{8\gamma_{\mathbf{k}}}{(\omega-2\omega_{\mathbf{k}})^2+4\gamma_{\mathbf{k}}^2}\,. \tag{3.15}$$

For sufficiently large ω and in the limit of small coupling (width) we may take $I(\omega,\mathbf{k}) \to 4\pi\delta(\omega - 2\omega_{\mathbf{k}})$ and the result of the previous calculation in the high-frequency region is recovered, as it should.

Let's now consider the low-frequency region, $\omega \lesssim m$. Here we may approximate $I(\omega,\mathbf{k}) \simeq 2\gamma_{\mathbf{k}}/\omega_{\mathbf{k}}^2$ and expand the difference between the Bose distributions to find

$$\rho_{\pi\pi}(\omega) = -\frac{8}{3}\int_{\mathbf{k}}\frac{|\mathbf{k}|^4}{\omega_{\mathbf{k}}^2}n'(\omega_{\mathbf{k}})\frac{\omega\gamma_{\mathbf{k}}}{\omega^2+4\gamma_{\mathbf{k}}^2} \qquad (0\le\omega\lesssim m)\,. \tag{3.16}$$

JHEP04(2002)053

We note that the last factor controls the pinch singularity in precise agreement with figure 1. Although in principle $\rho_{\pi\pi}(\omega)/T^4$ may depend on the three dimensionless combinations ω/T, γ/T, and m/T, we find that in practice it only depends on ω/γ and m/T. Since the integral is dominated by hard momenta the m/T dependence is subdominant and the natural parameter on which the spectral function depends in this region is ω/γ. It is easy to see that the spectral function has a local maximum at $\omega \sim \gamma$ and $\rho_{\pi\pi}(\omega \sim \gamma)/T^4 \sim 1$.

For very small frequencies $\omega \ll \gamma$ we expand and obtain

$$\frac{\rho_{\pi\pi}(\omega)}{T^4} = a_1\left(\frac{\omega}{\gamma}\right) + \frac{a_3}{3!}\left(\frac{\omega}{\gamma}\right)^3 + \cdots \quad (0 \le \omega \ll \gamma), \tag{3.17}$$

with

$$a_1 = -\frac{2}{3T^4}\int_{\mathbf{k}} \frac{|\mathbf{k}|^4}{\omega_{\mathbf{k}}^2} n'(\omega_{\mathbf{k}})\frac{\gamma}{\gamma_{\mathbf{k}}} \simeq \frac{5!\,\zeta(5)}{3\pi^2} \tag{3.18}$$

$$a_3 = \frac{1}{T^4}\int_{\mathbf{k}} \frac{|\mathbf{k}|^4}{\omega_{\mathbf{k}}^2} n'(\omega_{\mathbf{k}})\left(\frac{\gamma}{\gamma_{\mathbf{k}}}\right)^3 \simeq -\frac{7!\,\zeta(7)}{2\pi^2}, \tag{3.19}$$

where the $\simeq$ indicates that the final integrals are evaluated by neglecting the remaining momentum dependence of the damping rate (i.e. taking $B = 1$) as well as the thermal mass (the first approximation has numerically the largest effect). From this the one-loop viscosity follows as

$$\eta_{1-\mathrm{loop}} = -\frac{1}{30}\int_{\mathbf{k}} \frac{|\mathbf{k}|^4}{\omega_{\mathbf{k}}^2} n'(\omega_{\mathbf{k}})\frac{1}{\gamma_{\mathbf{k}}} \simeq \frac{2\zeta(5)}{\pi^2}\frac{T^4}{\gamma}. \tag{3.20}$$

However, as is well-known [3] these one-loop results are not complete and a ladder summation is required to obtain the complete leading-order result (see figure 3). Due to nearly pinching poles, each additional rung in the ladder contributes with a factor $\lambda^2 T/\gamma \sim 1$ and is therefore not suppressed. The effect of ladder summation is to change the coefficients $a_1, a_3, \ldots$, but not the parametric dependence on the coupling constant.

In the region $\gamma \ll \omega \lesssim m$ we find

$$\rho_{\pi\pi}(\omega)/T^4 = -\frac{8}{3T^4}\int_{\mathbf{k}} \frac{|\mathbf{k}|^4}{\omega_{\mathbf{k}}^2} n'(\omega_{\mathbf{k}})\frac{\gamma_{\mathbf{k}}}{\omega} \simeq \frac{8\zeta(3)}{\pi^2}\frac{\gamma}{\omega} \qquad (\gamma \ll \omega \lesssim m). \tag{3.21}$$

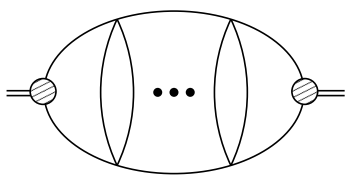

Figure 3: Ladder diagrams that contribute to $\rho_{\pi\pi}(\omega)$ in the scalar theory. In the low-frequency region, $\omega \lesssim \gamma$, the pinching-pole contributions from the ladder diagrams are equally important as the one-loop contribution. When $\omega \gg \gamma$, pinching-pole contributions from ladder diagrams are suppressed.

JHEP04(2002)053

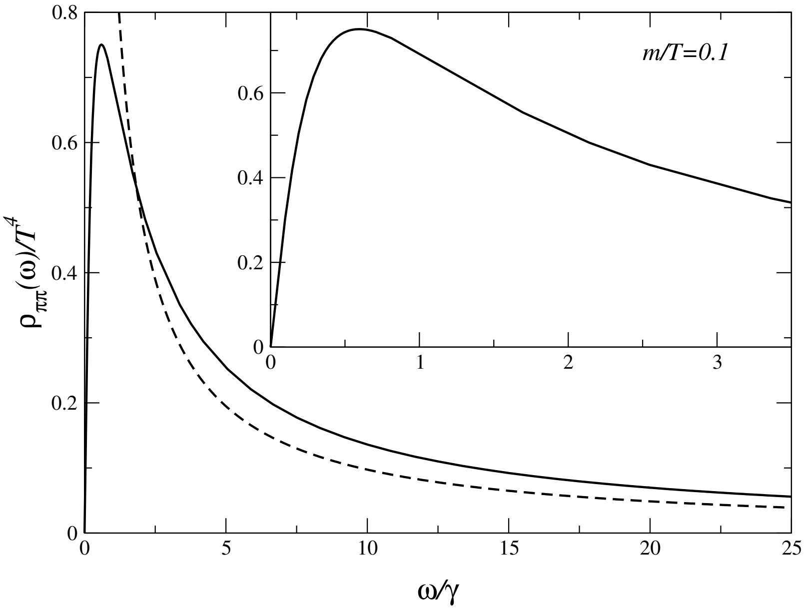

Figure 4: Contribution to the spectral function $\rho_{\pi\pi}(\omega)/T^4$ (full line) from the nearly pinching poles in the low-frequency region as a function of ω/γ, obtained by numerical integration of eq. (3.16). The dashed line is the analytical result (3.21) when $\gamma \ll \omega \lesssim m$, neglecting nontrivial momentum dependence and finite mass corrections. The inset shows a blowup. The viscosity is determined by the slope for $\omega \to 0$.

In this frequency interval pinching-pole contributions from ladders are subdominant since each additional rung comes with a factor $\lambda^2 T/\omega \ll 1$. The perturbative part of the three-loop ladder diagram (i.e. with a single rung) also contributes at this order and has the same $\lambda^2 T/\omega$ behaviour as we find above.[5] Figure 4 shows the contribution to the spectral function from the nearly pinching poles in the low-frequency interval, obtained by numerical integration of eq. (3.16) with the full momentum and mass dependence. Note that the natural dimensionless combinations in the low-frequency region differ from those in the high-frequency region (compare figures 2 and 4).

We may now combine the results obtained so far to construct the complete one-loop spectral function at high temperature in the weak-coupling limit. The spectral function can be written as the sum of the contributions discussed above:

$$\rho_{\pi\pi}(\omega) = \rho_{\pi\pi}^{\rm low}(\omega) + \rho_{\pi\pi}^{\rm high}(\omega)\,, \tag{3.22}$$

where $\rho_{\pi\pi}^{\rm low}$ represents the contribution from the nearly pinching poles in eq. (3.16), dominating at low frequencies, and $\rho_{\pi\pi}^{\rm high}$ is the contribution from decay/creation processes in eq. (3.7), dominating at higher frequencies.

We find that for very small frequencies the spectral function rises quickly as ω/γ. It reaches a maximum of order 1 (in units of temperature) at $\omega \sim \gamma$ and decays then slowly as γ/ω. Around the thermal mass the contribution from decay/creation processes enter

[5]We thank Guy Moore for pointing this out.

JHEP04(2002)053

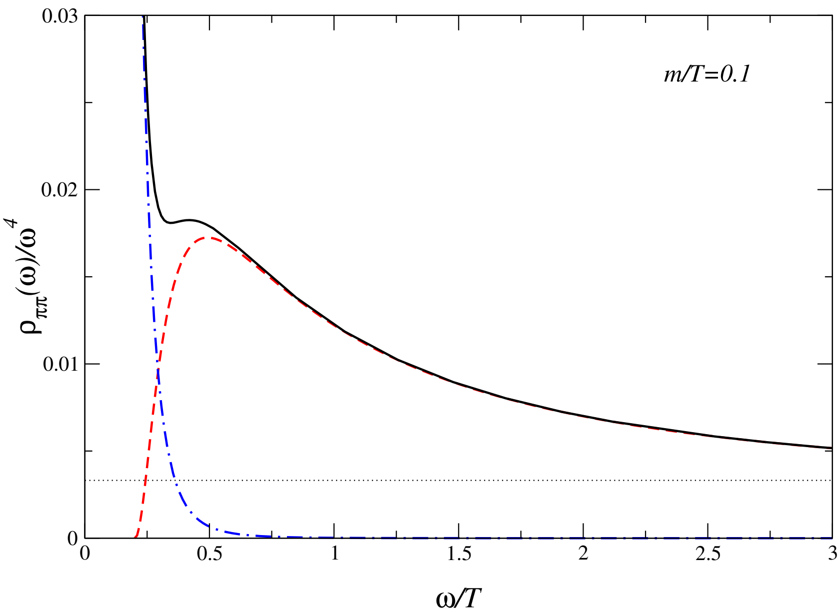

Figure 5: Complete one-loop spectral function $\rho_{\pi\pi}(\omega)/\omega^4$ (full line) as a function of ω/T, with $m/T = 0.1$. The dashed line is the contribution from decay/creation processes and vanishes below $\omega = 2m$, the dot-dashed line is the contribution due to the nearly pinching poles at lower frequencies. The dotted line indicates the asymptotic value.

and the spectral function increases again. Note that the results obtained in both frequency domains smoothly match parametrically at $\omega \sim m$, since $\rho_{\pi\pi}(\omega \sim 3m)/T^4 \sim \lambda^{3/2}$, both from the low- and the high-frequency calculation. For large ω the spectral function increases as ω^4, due to the zero-temperature decay process. Ladder diagrams do not affect this characteristic shape. In figure 5 we present the complete one-loop spectral function as a function of ω/T.[6] In order to combine the low- and the high-frequency contribution in one figure, we show $\rho_{\pi\pi}(\omega)/\omega^4$, which enhances the contribution at lower frequencies.

We are now ready to calculate the euclidean correlator using eq. (2.6). Because $G^E_{\pi\pi}(\tau)$ depends linearly on the spectral function, we write it as a sum of two contributions, $G^E_{\pi\pi} = G^{E,\rm low}_{\pi\pi} + G^{E,\rm high}_{\pi\pi}$, and discuss each term separately. We start with the contribution due to decay/creation processes which reads

$$G^{E,\rm high}_{\pi\pi}(\tau) = \int_{2m}^{\infty} \frac{d\omega}{2\pi}\, K(\tau,\omega) \frac{\left(\omega^2 - 4m^2\right)^{5/2}}{48\pi\omega} \left[n\left(\frac{\omega}{2}\right) + \frac{1}{2} \right]. \tag{3.23}$$

It is easy to see that the mass plays only a subdominant role and finite-mass corrections are suppressed by m^2/T^2. Therefore we take $m = 0$ which yields

$$G^{E,\rm high}_{\pi\pi}(\tau) = \frac{T^5}{96\pi^2} \int_0^{\infty} dx\, x^4 \left[e^{sx} + e^{(1-s)x} \right] n(x) \left[n\left(\frac{x}{2}\right) + \frac{1}{2} \right], \tag{3.24}$$

where $x = \omega/T$ and $s = \tau T$. The remaining integral can be performed and we find

$$G^{E,\rm high}_{\pi\pi}(\tau) = \frac{\pi^2 T^5}{3\sin^5 u} \left\{ (\pi - u) \left[11\cos u + \cos 3u \right] + 6\sin u + 2\sin 3u \right\}, \tag{3.25}$$

[6] We used here that $m/T = 0.1$ corresponds to $\lambda \simeq 0.267$ and $\gamma/T \simeq 1.48 \cdot 10^{-5}$.

JHEP04(2002)053

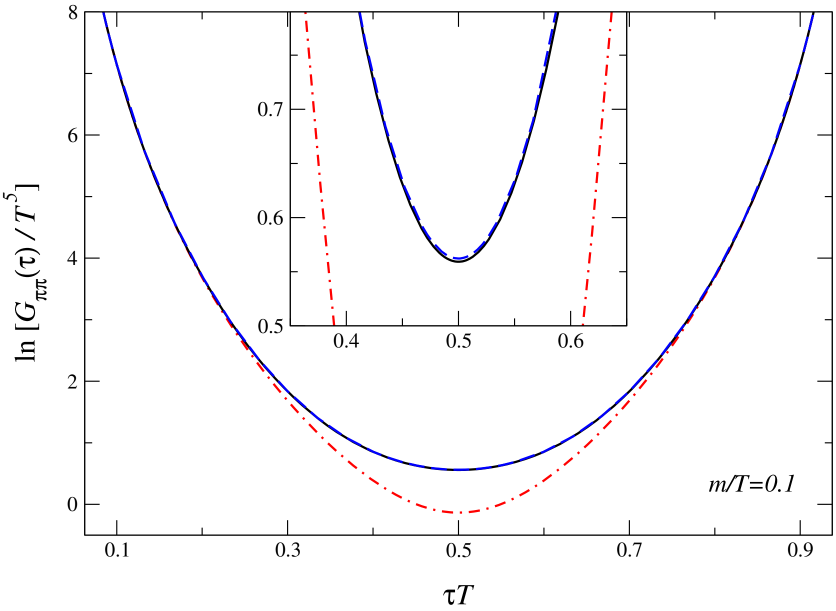

Figure 6: Logarithm of the euclidean correlator $G^E_{\pi\pi}(\tau)/T^5$ as a function of τT, obtained by numerical integration of eq. (2.6) with (3.22), for $m/T = 0.1$ (full line). The dashed line represents the analytical expression for $m = 0$, eq. (3.29); it cannot be distinguished from the full result, except in the inset. The dot-dashed line shows the contribution from decay/creation processes only, obtained by numerical integration of eq. (3.23). The inset shows a blowup around $\tau T = 0.5$.

where $u = 2\pi\tau T$. An approximate but illuminating expression for the euclidean correlator can be obtained by noticing that the integral in eq. (3.24) is dominated by hard frequencies, $x \gtrsim 1/s$ with $0 < s < 1$, such that the Bose distributions may be approximated with maxwellian ones, $n(x) \sim e^{-x}$. In that case we find

$$G^{E,\mathrm{high}}_{\pi\pi}(\tau) \simeq \frac{1}{8\pi^2}\left[\frac{1}{\tau^5} + \frac{1}{(1/T-\tau)^5} + \frac{2}{(3/2T-\tau)^5} + \frac{2}{(1/2T+\tau)^5}\right]. \qquad (3.26)$$

This approximate expression differs less than 2% from the exact result (3.25). The dominant $1/\tau^5$ behaviour of the correlator arises from decay at zero temperature. Finite temperature is manifested mainly through the reflection symmetry, $\tau \to 1/T - \tau$. At the central point $\tau T = 1/2$, we find the contribution to the euclidean correlator from the decay/creation processes to be

$$G^{E,\mathrm{high}}_{\pi\pi}(\tau = 1/2T) = \frac{4\pi^2}{45}T^5\left[1 - \frac{25}{8\pi^2}\frac{m^2}{T^2} + \cdots\right]. \qquad (3.27)$$

The effect of a finite mass is to lower the mimimal value of the correlator.

The contribution to the euclidean correlator from the nearly pinching poles in the low-frequency region can be found easily from eqs. (2.6) and (3.16) by interchanging frequency and momentum integrals. Since $\rho^{\mathrm{low}}_{\pi\pi}$ gives the dominant contribution to the spectral function up to frequencies of order m, whereas $\rho^{\mathrm{high}}_{\pi\pi}$ dominates for higher frequencies, we can

JHEP04(2002)053

use the expansion (2.9) for the kernel and obtain

$$\begin{aligned} G^{E,\mathrm{low}}_{\pi\pi}(\tau) &\simeq -\frac{8}{3}\int_{\mathbf{k}} \frac{|\mathbf{k}|^4}{\omega_{\mathbf{k}}^2} n'(\omega_{\mathbf{k}}) \int_0^{\omega_\Lambda} \frac{d\omega}{2\pi}\frac{2T}{\omega}\frac{\omega\gamma_{\mathbf{k}}}{\omega^2+4\gamma_{\mathbf{k}}^2} \\ &= -\frac{4}{3}\frac{T}{\pi}\int_{\mathbf{k}} \frac{|\mathbf{k}|^4}{\omega_{\mathbf{k}}^2} n'(\omega_{\mathbf{k}}) \arctan\left(\frac{\omega_\Lambda}{2\gamma_{\mathbf{k}}}\right) \\ &\simeq \frac{4\pi^2}{45}T^5\left[1-\frac{25}{8\pi^2}\frac{m^2}{T^2}+\cdots\right], \end{aligned} \tag{3.28}$$

with $\omega_\Lambda \sim m$. The error that is introduced by expanding the kernel is negligible (see figure 6). We note that in our one-loop calculation this result is at leading order independent of the coupling constant. Similarly, while ladder diagrams determine the precise shape of the spectral function, the effect on the euclidean correlator $G^{E,\mathrm{low}}_{\pi\pi}(\tau)$ appears only in subleading corrections in the coupling constant, as can be seen with the kinetic approach [18]. Therefore the low-frequency contribution to the euclidean correlator is constant and of order one (in the appropriate units) and insensitive to details of the ladder summation.

Combining the low- and high-frequency contribution to the euclidean correlator at high temperature and weak coupling we find, to leading order in the coupling constant,

$$G^E_{\pi\pi}(\tau) = \frac{\pi^2 T^5}{3\sin^5 u}\left\{(\pi-u)\left[11\cos u+\cos 3u\right]+6\sin u+2\sin 3u\right\}+\frac{4\pi^2}{45}T^5\,, \tag{3.29}$$

with $u = 2\pi\tau T$. Corrections due to the finite thermal mass are suppressed by m^2/T^2. The euclidean correlator is minimal at $\tau T = 1/2$, and $G^E_{\pi\pi}(1/2T)$ receives contributions of the same order from both the high- and the low-frequency region (at leading order in the coupling they are equal). A comparison between the analytical result at $m = 0$ and the full result obtained by numerical integration of eq. (2.6) with eq. (3.22) in the presence of a finite mass is shown in figure 6.

4. Nonabelian gauge fields

We leave the scalar case and consider nonabelian $SU(N_c)$ gauge theory. The traceless spatial part of the energy-momentum tensor is

$$\pi_{ij} = F_i^{a\mu}F^a_{j\mu} - \frac{1}{3}\delta_{ij}F^{ak\mu}F^a_{k\mu}\,. \tag{4.1}$$

The coupling vertex between the operator π_{ij} and two gluons with incoming momenta P, K and indices $(\mu, a), (\nu, b)$ respectively can be read from (4.1) and we find[7]

$$\begin{aligned} \Gamma^{ab}_{ij,\mu\nu}(P,K) = -\delta^{ab}\Bigg[&\delta_{\mu\nu}\left(p_ik_j+p_jk_i-\frac{2}{3}\delta_{ij}\mathbf{p}\cdot\mathbf{k}\right)+P\cdot K\left(\delta_{i\mu}\delta_{j\nu}+\delta_{i\nu}\delta_{j\mu}-\frac{2}{3}\delta_{ij}\delta_{k\mu}\delta_{k\nu}\right)- \\ &-\left(p_iK_\mu\delta_{j\nu}+p_jK_\mu\delta_{i\nu}+P_\nu k_i\delta_{j\mu}+P_\nu k_j\delta_{i\mu}\right)+ \\ &+\frac{2}{3}\delta_{ij}\left(P_\nu k_k\delta_{k\mu}+p_kK_\mu\delta_{k\nu}\right)\Bigg]\,. \end{aligned} \tag{4.2}$$

[7] In order to arrive at the basic one-loop expression (4.5) below we use here the imaginary-time formalism with $P = (p_4, \mathbf{p})$, the Matsubara frequency $\omega_n = -p_4 = 2\pi nT$ $(n \in \mathbb{Z})$ and $P\cdot K = p_4k_4 + \mathbf{p}\cdot\mathbf{k}$.

JHEP04(2002)053

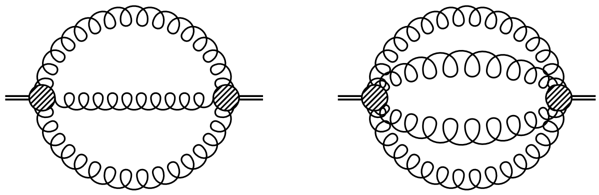

Figure 7: Diagrams that contribute to the spectral function $\rho_{\pi\pi}$ at higher order. These diagrams are special for a nonabelian theory.

In the nonabelian theory π_{ij} also couples to three and four gluons, which leads to diagrams as depicted in figure 7. However, these contributions are suppressed by powers of the coupling constant and will not be considered further.

We use the Coloumb gauge in which the gluon propagator reads

$$D_{\mu\nu}(P) = \mathcal{P}^T_{\mu\nu}(\hat{\mathbf{p}})\Delta_T(P) + \delta_{4\mu}\delta_{4\nu}\Delta_L(P)\,, \tag{4.3}$$

with $\mathcal{P}^T_{ij}(\hat{\mathbf{p}}) = \delta_{ij} - \hat{p}_i\hat{p}_j$, $\mathcal{P}^T_{4\mu} = \mathcal{P}^T_{\mu 4} = 0$. The transverse and longitudinal components have the following spectral representations

$$\Delta_T(P) = -\int_{-\infty}^{\infty}\frac{d\omega}{2\pi}\,\frac{\rho_T(\omega,\mathbf{p})}{i\omega_n - \omega}\,, \qquad \Delta_L(P) = \frac{1}{\mathbf{p}^2} + \int_{-\infty}^{\infty}\frac{d\omega}{2\pi}\,\frac{\rho_L(\omega,\mathbf{p})}{i\omega_n - \omega}\,. \tag{4.4}$$

The one-loop contribution to the spectral function reads, after evaluating the Matsubara sum and taking all frequencies real again,

$$\begin{aligned}\rho_{\pi\pi}(\omega) = \frac{2d_A}{3}\int\frac{d^4k}{(2\pi)^4}\left[n(k^0) - n(k^0+\omega)\right]\Big\{&V_1(k,\omega)\rho_T(k^0,\mathbf{k})\rho_T(k^0+\omega,\mathbf{k}) + \\ &+ V_2(k)\rho_T(k^0,\mathbf{k})\rho_L(k^0+\omega,\mathbf{k}) + \\ &+ V_3(\mathbf{k})\rho_L(k^0,\mathbf{k})\rho_L(k^0+\omega,\mathbf{k})\Big\}\,,\end{aligned} \tag{4.5}$$

where $d_A = N_c^2 - 1$ is the number of gluons and $V_1(k,\omega) = 7|\mathbf{k}|^4 - 10\mathbf{k}^2k^0(k^0+\omega) + 7(k^0)^2(k^0+\omega)^2$, $V_2(k) = 6\mathbf{k}^2(k^0)^2$ and $V_3(\mathbf{k}) = -32|\mathbf{k}|^4$. This expression is the equivalent of eq. (3.5) in the scalar theory.

As in the scalar case, we start the analysis for external frequencies ω that are sufficiently large such that no pinch singularities are present. The collective (HTL) effects in a nonabelian plasma [19] can be incorporated in the one-particle spectral functions, which are however more complex than in the scalar case. The spectral function for transverse gluons can be written as [20, 21]

$$\rho_T(k^0,\mathbf{k}) = 2\pi Z_T(|\mathbf{k}|)\left\{\delta[k^0 - \omega_T(|\mathbf{k}|)] - \delta[k^0 + \omega_T(|\mathbf{k}|)]\right\} + \beta_T(k^0,|\mathbf{k}|)\,. \tag{4.6}$$

The delta functions describe propagating quasiparticles with a dispersion relation ω_T and a residue

$$Z_T(k) = \frac{\omega_T(k)[\omega_T^2(k) - k^2]}{3\omega_{\rm pl}^2\omega_T^2(k) - [\omega_T^2(k) - k^2]^2}\,, \tag{4.7}$$

JHEP04(2002)053

where $\omega_{\rm pl}^2 = g^2T^2N_c/9$ is the plasma frequency squared. For small and large spatial momentum one finds

$$\begin{aligned}
\omega_T^2(k) &\simeq \omega_{\rm pl}^2 + \frac{6}{5}k^2\,, \qquad Z_T(k) \simeq \frac{1}{(2\omega_{\rm pl})} \quad (k \to 0)\,, \\
\omega_T^2(k) &\simeq k^2 + m_\infty^2\,, \qquad Z_T(k) \simeq \frac{1}{(2k)} \quad (k \to \infty)\,,
\end{aligned} \tag{4.8}$$

where $m_\infty^2 = \frac{3}{2}\omega_{\rm pl}^2$ is the asymptotic gluon mass squared. The β_T function describes Landau damping and is nonzero below the light-cone only. The spectral function of longitudinal gluons $\rho_L(k^0, \mathbf{k})$ has a similar form [20, 21].

We start studying the contribution to eq. (4.5) when both gluons are transverse. There are three parts, depending on whether we take from the one-particle spectral functions the delta functions of the quasiparticles (pole-contribution) or the β function of the Landau damping (cut-contribution). When both gluons are quasiparticles the integrals can be done with the help of the delta functions and we find the pole-pole contribution for transverse gluons

$$\rho_{\pi\pi}^{\rm pp}(\omega) = \theta(\omega - 2\omega_{\rm pl})\frac{2d_A}{3\pi}\frac{Z_T^2(f_0)f_0^2}{\omega_T'(f_0)}\left(7f_0^4 + \frac{5}{2}f_0^2\omega^2 + \frac{7}{16}\omega^4\right)\left[n\left(\frac{\omega}{2}\right) + \frac{1}{2}\right]. \tag{4.9}$$

Here we use the notation $f_0 = f(\omega/2)$, with $f(u)$ defined as the inverse of the transverse dispersion relation, $f[\omega_T(k)] = k$. The function $f(u)$ vanishes when $u \le \omega_{\rm pl}$, and

$$\begin{aligned}
f(u) &\simeq \sqrt{\frac{5}{6}(u^2 - \omega_{\rm pl}^2)} \qquad (u \to \omega_{\rm pl})\,, \\
f(u) &\simeq u - \frac{3\omega_{\rm pl}^2}{4u} \qquad (u \to \infty)\,.
\end{aligned} \tag{4.10}$$

Again, as for the scalar case, the HTL resummation produces the threshold in the spectral function (4.9) for soft external frequency. We find that

$$\rho_{\pi\pi}^{\rm pp}(\omega \sim gT) \sim g^3T^4\,. \tag{4.11}$$

For large ω the spectral function behaves as

$$\rho_{\pi\pi}^{\rm pp}(\omega) = \frac{d_A}{4\pi}\omega^4\left[n\left(\frac{\omega}{2}\right) + \frac{1}{2}\right] \qquad (\omega \gg \omega_{\rm pl})\,, \tag{4.12}$$

which is, up to the prefactor, what we found in the scalar case as well.

The contribution when one transverse gluon is a quasiparticle and the other undergoes Landau damping (pole-cut contribution) is

$$\begin{aligned}
\rho_{\pi\pi}^{\rm pc}(\omega) = \frac{2d_A}{3\pi^2}\int_{\omega_{\rm pl}}^{\infty} du\,\frac{f^2(u)}{\omega_T'[f(u)]}Z_T[f(u)][n(u-\omega) - n(u)]\beta_T[u-\omega, f(u)] \times \\
\times\left[7f^4(u) - 10u(u-\omega)f^2(u) + 7u^2(u-\omega)^2\right].
\end{aligned} \tag{4.13}$$

For soft $\omega \sim gT$ the dominant contribution arises when the energy u is hard, and we may use

$$\beta_T[u-\omega, f(u)] \sim \frac{3\pi}{4}\frac{\omega_{\rm pl}^2}{\omega u^3}\,, \tag{4.14}$$

JHEP04(2002)053

as well as other simplifications given above. We find

$$\rho_{\pi\pi}^{\rm pc}(\omega\sim gT)\simeq-\frac{d_A}{\pi}\omega_{\rm pl}^2\int_{\omega_{\rm pl}}^{\infty}du\,u^2n'(u)\sim g^2T^4\,. \tag{4.15}$$

For soft external frequencies the pole-cut contribution dominates over the pole-pole contribution (4.11).

For hard frequencies $\omega\sim T$, the β_T function determines the lower integration limit to be $u_0=\omega/2+3\omega_{\rm pl}^2/(4\omega)$. As a result, u is always hard and we can simplify the integrand to arrive at

$$\rho_{\pi\pi}^{\rm pc}(\omega\sim T)=\frac{d_A}{3\pi^2}\int_{u_0}^{\infty}du\,u^3\left(4u^2-4u\omega+7\omega^2\right)[n(u-\omega)-n(u)]\beta_T(u-\omega,u)\,. \tag{4.16}$$

It is convenient to substitute $u=\omega(z+1)/2$ such that

$$\rho_{\pi\pi}^{\rm pc}(\omega\sim T)=\frac{d_A\omega^6}{48\pi^2}\int_{a}^{\infty}dz\,(z+1)^3\left(z^2+6\right)[n(\omega z_-)-n(\omega z_+)]\beta_T(\omega z_-,\omega z_+)\,, \tag{4.17}$$

where $z_\pm=(z\pm1)/2$ and $a=3\omega_{\rm pl}^2/(2\omega^2)$. The dominant contribution comes from the lower integration limit ($z\to a$) where the β_T function can be approximated as

$$\beta_T(\omega z_-,\omega z_+)\simeq-\frac{4\pi}{\omega^2}\frac{za}{(z+a)^2}\,. \tag{4.18}$$

Using this expression we find that

$$\rho_{\pi\pi}^{\rm pc}(\omega\sim T)\sim g^2T^4\ln\left(\frac{1}{g}\right). \tag{4.19}$$

For hard frequencies the pole-cut contribution is therefore suppressed compared to the pole-pole contribution (4.12). Finally, we found that the remaining cut-cut contribution when both gluons are transverse is suppressed with respect to the pole-pole contribution when ω is hard and to the pole-cut contribution when ω is soft.

In a similar way we have analysed the remaining longitudinal-transverse and longitudinal-longitudinal contributions in eq. (4.5) with the result that they do not modify the conclusions drawn from the transverse-transverse contribution analysed above. In particular, for hard frequencies $\omega\gg\omega_{\rm pl}$ transverse gluons dominate and the spectral function is given by eq. (4.12). We do not need to be more explicit about the region where $\omega\lesssim gT$ because the dominant contribution in this region arises from the pinching poles, screened by a finite width and/or external frequency, as we will show now.

For small external frequencies $0\leq\omega\lesssim gT$ the loop integral is dominated by the region of hard momentum and we only need to consider transverse gluons, since the residue for longitudinal gluons vanishes exponentially. In order to avoid pinch singularities we follow the same steps as in the scalar case and substitute for the one-particle spectral function a Breit-Wigner function, see eq. (3.8). For transverse on-shell gluons with hard momentum the dispersion relation is $\omega_{\mathbf{k}}=\sqrt{\mathbf{k}^2+m_\infty^2}$ and the leading (momentum-independent) contribution to the damping rate is [22]

$$\gamma=\frac{g^2}{4\pi}N_cT\ln\left(\frac{1}{g}\right), \tag{4.20}$$

JHEP04(2002)053

where the logarithm is sensitive to the magnetic mass, $\ln(\omega_{\rm pl}/m_{\rm mag}) \sim \ln(1/g)$ with $m_{\rm mag} \sim g^2T$.[8] The mass m_∞ only plays a subdominant role and is neglected below. Evaluating the integral over k^0 exactly as in the scalar case, we find

$$\rho_{\pi\pi}(\omega) = -\frac{d_A}{3}\int_{\mathbf{k}}\frac{1}{|\mathbf{k}|}\left\{[n(|\mathbf{k}|)-n(|\mathbf{k}|-\omega)]I(\omega,\mathbf{k})A(\omega,\mathbf{k})\frac{|\mathbf{k}|-\omega}{\omega^2+4\gamma^2}-[\omega\to-\omega]\right\}, \quad (4.21)$$

where $I(\omega,\mathbf{k})$ was defined in eq. (3.15) and $A(\omega,\mathbf{k}) = \mathbf{k}^2\left(4\mathbf{k}^2-4\omega|\mathbf{k}|+7\omega^2\right)$. For $\omega \lesssim \omega_{\rm pl}$ this expression simplifies to

$$\rho_{\pi\pi}(\omega) = -\frac{16d_A}{3}\int_{\mathbf{k}}\mathbf{k}^2n'(|\mathbf{k}|)\frac{\omega\gamma}{\omega^2+4\gamma^2} \qquad (0\le\omega\lesssim\omega_{\rm pl}), \quad (4.22)$$

which is $2d_A$ times the scalar result. In the region $\gamma \ll \omega \lesssim \omega_{\rm pl}$ we find

$$\frac{\rho_{\pi\pi}(\omega)}{T^4} = -\frac{16d_A}{3T^4}\frac{\gamma}{\omega}\int_{\mathbf{k}}\mathbf{k}^2n'(|\mathbf{k}|) = \frac{32\pi^2}{45}d_A\frac{\gamma}{\omega}. \quad (4.23)$$

As in the scalar case, the three-loop ladder diagram with one rung contributes in this region at the same order. Note that the contribution from the pinching poles at $\omega \sim gT$,

$$\rho_{\pi\pi}(\omega\sim gT) \sim gT^4\ln\left(\frac{1}{g}\right) \quad (4.24)$$

actually dominates over the contribution (4.15) from the collective (HTL) excitations in this region. The shear viscosity in the one-loop approximation follows from (4.22) as

$$\eta_{1-\rm loop} = \frac{8\pi^2d_A}{225}\frac{T^4}{\gamma}. \quad (4.25)$$

However, for the complete spectral function at small frequencies $0 \le \omega \lesssim \gamma$ the effects of ladder diagrams must be taken into account. As was mentioned in the Introduction, kinetic theory predicts that the shear viscosity is parametrically larger than the one-loop result (4.25) [7, 8, 24]. Therefore, for vanishing frequency the spectral function due to ladder diagrams is expected to be larger than the one-loop contribution and to behave as $\rho_{\pi\pi}^{\rm ladder}(\omega\to0) = 20\eta\,\omega$, with [8]

$$\eta \sim \frac{N_c^2-1}{N_c^2}\frac{T^3}{g^4\ln(1/g)}. \quad (4.26)$$

Hence the slope of the spectral function is much steeper close to the origin, compared to the one-loop result. Up to frequencies $\omega \sim \gamma$ the actual behaviour of the spectral function depends on the pinching-poles contribution of ladders diagrams. When $\gamma \ll \omega \lesssim \omega_{\rm pl}$ pinching-poles contributions of the ladders are subdominant by a factor g^2T/ω and the spectral function decreases as g^2T/ω until it meets with the rising contribution from eq. (4.12). For large ω the spectral function increases as ω^4.

The euclidean correlator at high temperature can be computed as in the scalar case and we find, at leading order in g,

$$G^E_{\pi\pi}(\tau)/T^5 = \frac{4\pi^2d_A}{\sin^5u}\left\{(\pi-u)\left[11\cos u+\cos 3u\right]+6\sin u+2\sin 3u\right\}+\frac{8\pi^2d_A}{45}, \quad (4.27)$$

with $u = 2\pi\tau T$. The last constant term reflects the low-frequency region.

[8]In QED there is no magnetic mass which could regularize the logarithmic divergence of the leading contribution to the damping rate. It turns out that the electron damping rate is ill defined [23].

JHEP04(2002)053

5. Conclusions

We have studied the spectral function relevant for the shear viscosity in scalar and nonabelian gauge theories at high temperature as a function of the external frequency. While for small frequencies ladder diagrams are important in the scalar case and essential in the nonabelian case, for higher frequencies a simple one-loop computation yields the dominant contribution.

We found that the spectral function has a characteristic shape: for small frequencies the spectral function rises, reaches a local maximum and decreases as $1/\omega$. This contribution is due to scattering processes in the plasma and is enhanced due to nearly pinching poles. We referred to this contribution as the low-frequency contribution. For higher frequencies, decay/creation processes dominate and the spectral function increases essentially as ω^4. This contribution is referred to as the high-frequency contribution.

In order to extract transport coefficients from euclidean lattice correlators, a simple ansatz, essentially a Breit-Wigner spectral function, was introduced in ref. [9] to model spectral functions of components of the energy-momentum tensor. The resulting three-parameter ansatz was subsequently used in refs. [13, 14] to determine transport coefficients in hot gauge theories from lattice simulations. Unfortunately, as we have seen in this paper, at high temperature spectral functions of composite operators do not resemble simple Breit-Wigner functions at all. In order to improve this analysis, we propose therefore to use a different ansatz, which is written as the sum of two terms:

$$\rho_{\pi\pi}(\omega) = \rho_{\pi\pi}^{\text{low}}(\omega) + \rho_{\pi\pi}^{\text{high}}(\omega) \,. \tag{5.1}$$

The high-frequency part can be described by eqs. (4.12) or (3.7) with m as a possible free parameter. For the low-frequency part we note that the spectral function is odd, increases linearly with ω for small ω and decreases with $1/\omega$ for larger ω. A simple ansatz reflecting this is

$$\rho_{\pi\pi}^{\text{low}}(x)/T^4 = x\frac{b_1 + b_2x^2 + b_3x^4 + \cdots}{1 + c_1x^2 + c_2x^4 + c_3x^6 + \cdots}\,, \qquad x = \frac{\omega}{T}\,, \tag{5.2}$$

with $b_i = c_i = 0$, $i > n$ for given n. The viscosity is given by $\eta/T^3 = b_1/20$. The ansatz (5.1), with free parameters m, b_i, and c_i, should be used in eq. (2.6) to fit the corresponding euclidean correlator to the numerical results. When insisting on a three-parameter fit, one may take $n = 1$ which leaves m, b_1 and c_1 to be determined.

Concerning the euclidean correlator, we found that the dominant τ dependence is determined by the high-frequency part ($\omega \gtrsim T$) of the spectral function. However, around $\tau T = 1/2$ both the high- and the low-frequency regions of the spectral function contribute at the same order. The low-frequency contribution is of special importance since transport coefficients are determined by the slope of the spectral function at zero frequency and a precise calculation of the spectral function at low frequencies is therefore essential. We found that no matter how complicated the spectral function up to frequencies $\omega \sim gT$ ($g \ll 1$) might be, its contribution to the euclidean correlator will be a τ independent constant. This latter feature poses a severe challenge for the MEM approach, since the spectral function at low frequencies should be reconstructed from the knowledge of a single constant

JHEP04(2002)053

alone. It turns out that this constant carries information on the transport coefficient (or more generally on ladder diagrams) only in subleading contributions. As a result euclidean correlators are remarkably insensitive to transport coefficients, which makes it extremely difficult to extract those at weak coupling.

We emphasize that these results are not specific for the correlator we considered here. For instance, in the first paper of ref. [10] the current-current correlator relevant for thermal dilepton rates in QCD was studied on the lattice and an enhancement in the central value of the euclidean correlator compared to the free result was observed. This enhancement might be accounted for by the pinching-poles contribution in the low-frequency region of the spectral function.[9]

Acknowledgments

It is a pleasure to thank Ulrich Heinz and Eric Braaten for discussions and comments. G.A. thanks Jan Smit and Nucu Stamatescu as well. We thank Guy Moore for a careful reading of and valuable comments on the manuscript. G.A. is supported by the Ohio State University through a Postdoctoral Fellowship and by the U.S. Department of Energy under Contract No. DE-FG02-01ER41190. J.M.M.R. is supported by a Postdoctoral Fellowship from the Basque Government.

References

[1] For ideal hydrodynamics, see e.g., P.F. Kolb, U.W. Heinz, P. Huovinen, K.J. Eskola and K. Tuominen, *Centrality dependence of multiplicity, transverse energy and elliptic flow from hydrodynamics*, *Nucl. Phys.* **A 696** (2001) 197 [`hep-ph/0103234`];
D. Teaney, J. Lauret and E.V. Shuryak, *A hydrodynamic description of heavy ion collisions at the SPS and RHIC*, `nucl-th/0110037`, and references therein.

[2] A. Muronga, *Second order dissipative fluid dynamics for ultra-relativistic nuclear collisions*, *Phys. Rev. Lett.* **88** (2002) 062302 [`nucl-th/0104064`].

[3] S. Jeon, *Hydrodynamic transport coefficients in relativistic scalar field theory*, *Phys. Rev.* **D 52** (1995) 3591 [`hep-ph/9409250`].

[4] S. Jeon and L.G. Yaffe, *From quantum field theory to hydrodynamics: transport coefficients and effective kinetic theory*, *Phys. Rev.* **D 53** (1996) 5799 [`hep-ph/9512263`].

[5] E. Wang and U.W. Heinz, *Nonperturbative calculation of the shear viscosity in hot Φ^4 theory in real time*, *Phys. Lett.* **B 471** (1999) 208 [`hep-ph/9910367`]; *Shear viscosity of hot scalar field theory in the real-time formalism*, `hep-th/0201116`.

[6] J.M. Martínez Resco and M.A. Valle Basagoiti, *Color conductivity and ladder summation in hot QCD*, *Phys. Rev.* **D 63** (2001) 056008 [`hep-ph/0009331`].

[7] R.D. Pisarski, *Medley in finite temperature field theory*, `hep-ph/9302241`.

[8] P. Arnold, G.D. Moore and L.G. Yaffe, *Transport coefficients in high temperature gauge theories, 1. Leading-log results*, *J. High Energy Phys.* **11** (2000) 001 [`hep-ph/0010177`].

[9] Note, however, that in the lattice study the spectral function reconstructed with the Maximal Entropy Method seems to vanish below $\omega \sim 3T$.

JHEP04(2002)053

[9] F. Karsch and H.W. Wyld, *Thermal Green's functions and transport coefficients on the lattice*, *Phys. Rev.* **D 35** (1987) 2518.

[10] F. Karsch, E. Laermann, P. Petreczky, S. Stickan and I. Wetzorke, *A lattice calculation of thermal dilepton rates*, *Phys. Lett.* **B 530** (2002) 147 [hep-lat/0110208];
I. Wetzorke, F. Karsch, E. Laermann, P. Petreczky and S. Stickan, *Meson spectral functions at finite temperature*, *Nucl. Phys.* **106** *(Proc. Suppl.)* (2002) 510 [hep-lat/0110132];
Temporal quark and gluon propagators: measuring the quasiparticle masses, *Nucl. Phys.* **106** *(Proc. Suppl.)* (2002) 513 [hep-lat/0110111];
For an early study, see QCD-TARO collaboration, P. de Forcrand et al., *Spectral analysis*, *Nucl. Phys.* **98** *(Proc. Suppl.)* (1998) 460.

[11] For zero temperature, see M. Asakawa, T. Hatsuda and Y. Nakahara, *Maximum entropy analysis of the spectral functions in lattice QCD*, *Prog. Part. Nucl. Phys.* **46** (2001) 459 [hep-lat/0011040];
CP-PACS collaboration, T. Yamazaki et al., *Spectral function and excited states in lattice QCD with maximum entropy method*, *Phys. Rev.* **D 65** (2002) 014501 [hep-lat/0105030].

[12] G. Aarts, *Spectral function at high temperature in the classical approximation*, *Phys. Lett.* **B 518** (2001) 315 [hep-ph/0108125];
Spectral function at high temperature, *Nucl. Phys.* **106** *(Proc. Suppl.)* (2002) 534 [hep-lat/0109024].

[13] A. Nakamura, S. Sakai and K. Amemiya, *Transport coefficients of quark gluon plasma for pure gauge models*, *Nucl. Phys.* **53** *(Proc. Suppl.)* (1997) 432 [hep-lat/9608052].

[14] A. Nakamura, T. Saito and S. Sakai, *Numerical results for transport coefficients of quark gluon plasma with Iwasaki's improved action*, *Nucl. Phys.* **63** *(Proc. Suppl.)* (1998) 424 [hep-lat/9710010]; *Transport coefficients of quark gluon plasma from lattice gauge theory*, *Nucl. Phys.* **A 638** (1998) 535 [hep-lat/9810031]; *Anisotropic lattice and its application to quark gluon plasma*, *Nucl. Phys.* **106** *(Proc. Suppl.)* (2002) 543 [hep-lat/0110177].

[15] R.R. Parwani, *Resummation in a hot scalar field theory*, *Phys. Rev.* **D 45** (1992) 4695 [hep-ph/9204216], erratum *ibid.* **D 48** (1992) 5965.

[16] E.-K. Wang and U.W. Heinz, *The plasmon in hot ϕ^4 theory*, *Phys. Rev.* **D 53** (1996) 899 [hep-ph/9509333].

[17] E.-K. Wang, U.W. Heinz and X.-F. Zhang, *Spectral functions for composite fields and viscosity in hot scalar field theory*, *Phys. Rev.* **D 53** (1996) 5978 [hep-ph/9509331].

[18] Guy Moore, private communication.

[19] E. Braaten and R.D. Pisarski, *Soft amplitudes in hot gauge theories: a general analysis*, *Nucl. Phys.* **B 337** (1990) 569.

[20] M. Le Bellac, *Thermal field theory*, Cambridge University Press, Cambridge 1996.

[21] J.-P. Blaizot and E. Iancu, *The quark-gluon plasma: collective dynamics and hard thermal loops*, *Phys. Rept.* **359** (2002) 355 [hep-ph/0101103].

[22] R.D. Pisarski, *Damping rates for moving particles in hot QCD*, *Phys. Rev.* **D 47** (1993) 5589.

[23] J.-P. Blaizot and E. Iancu, *Lifetimes of quasiparticles and collective excitations in hot QED plasmas*, *Phys. Rev.* **D 55** (1997) 973 [hep-ph/9607303].

[24] G. Baym, H. Monien, C.J. Pethick and D.G. Ravenhall, *Transverse interactions and transport in relativistic quark-gluon and electromagnetic plasmas*, *Phys. Rev. Lett.* **64** (1990) 1867.

JHEP04(2002)053